

Push the Limit of Acoustic Indoor Fire Monitoring

Zheng Wang^{†‡}, Xiaoqi Sun[†], Yuanqing Zheng[¶], Yanwen Wang^{†§}

[†]Hunan University, China [‡]China Electric Power Research Institute, China

[§]Shenzhen Research Institute, Hunan University, China [¶]The Hong Kong Polytechnic University, Hong Kong, China

{wangzheng, sunxiaoqi}@hnu.edu.cn csyqzheng@comp.polyu.edu.hk wangyw@hnu.edu.cn

Abstract—In indoor fire rescue, swift and precise fire source localization and fire severity assessment are pivotal for firefighting strategic planning and casualty evacuation. However, existing solutions primarily focus on detecting fire presence, which do not offer insights into fire's localization and severity. In this paper, we propose UltraFlame, an accurate, user-friendly, and timely system for pinpointing fire sources and assessing fire severity based on acoustic sensing, which bridges significant gaps in fire safety and response. UltraFlame consists of a collocated commodity speaker and microphone pair, sensing fire by emitting inaudible sound waves. We conduct an in-depth investigation of sound propagation impacted by fire combustion, providing physically interpretable data for deep learning framework and enabling fire source localization even without any sound reflection by fire. We dedicatedly establish a correlation between fire severity and sound propagation delays, which serves as an effective indicator for estimating the heated region. Finally, an appropriate deep learning framework is employed to effectively extract temporal and spatial features from channel measurement. Extensive experiments demonstrate that 94% of the localization results have an error of less than 0.8m. Additionally, UltraFlame achieves an accuracy of 96.9% in fire severity assessment across diverse setups, providing real-time and reliable monitoring.

Index Terms—Acoustic sensing, channel impulse response, fire source localization, fire severity assessment

I. INTRODUCTION

Motivation. In indoor fire rescue operations, every minute counts and every life matters. Merely detecting the presence of a flame is far from sufficient to meet the requirements of modern fire rescue systems, as shown in Fig. 1. In high-density residential buildings, the lack of precise fire localization can lead to mass panic, posing difficulties for firefighters in quickly and effectively enacting fire rescue strategies and planning evacuation routes. Transportation hubs require rapid fire source localization to ensure passenger safety and control the fire spreading. Moreover, industrial hazardous materials demand for immediate and accurate fire severity estimation to prevent disasters. Power supply rooms, educational institutions, data centers, and other indoor facilities all face unique challenges, and simply knowing the occurrence of a fire event is not enough to address these issues. Furthermore, simply detecting the fire at the room level is insufficient for automatic firefighting robots to extinguish fires quickly and precisely at specific locations.

Prior works and limitations. Existing fire monitoring approaches are limited to mere detection of fire presence, which commonly rely on smoke detectors [6], [8], [25], [29], such as photoelectric sensors [8], ionization sensors [29], and



(a) Real-time monitoring and dynamic planning.
(b) Embodied intelligence robots for precise fire extinguishing.
(c) Accurate assessment of fire severity.

Fig. 1. Fire incidents and rescue responses. (Generated by ChatGPT 4.0)

gas sensor [8], enabling early warnings and timely detection of smoke. However, these sensors only trigger alarms when certain thresholds are exceeded, which lacks the information of fire's location and severity. Deploying multiple infrared sensors enables fire source localization, while still struggling with assessing fire severity and facing challenges when the fire sources are obstructed [1]. In vision-based methods, it is challenging to locate fire source and assess fire severity if cameras are contaminated or obscured by smoke particles [23]. Wireless signal-based fire monitoring methods have attracted attention in recent years [11], [12], [16]–[18], [26], [37], [39]. Recent researchers employ Radio Frequency (RF) technology to detect the presence of smoke. The intuition is that smoke particles impact the RF signal propagation paths, causing changes in signal strength [16], [26], [39]. However, the RF-based method entails long processing delay to output a fire's location [26], which is hard to satisfy real-time requirement of fire monitoring systems.

Recent years have witnessed a surge of acoustic-based sensing technologies [3], [21], [24], [33]–[36], [38]. In fire monitoring, microphones have been employed to passively capture sound generated by flame combustion [21], [24]. By analyzing the frequency and amplitude of the sound during combustion, it is possible to determine fire source location and assess its severity. However, passive fire monitoring only using microphones is susceptible to environmental noises [21]. Different from passive acoustic sensing techniques, active probing fire is superior in stronger controllability, inaudibility, and signal processing advantages, potentially enhancing detection accuracy and reliability. AcousticThermo proactively emits an acoustic pulse signal to measure air temperature by calculating sound propagation speed [38]. However, AcousticThermo entails precise system initialization to obtain the round-trip distance of sound signal before use, which is difficult or even

Yanwen Wang is the corresponding author.

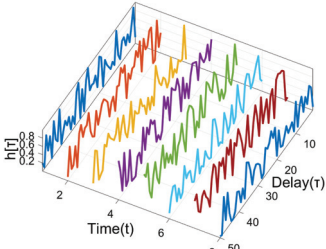


Fig. 2. CIR shown in a 3-D matrix.

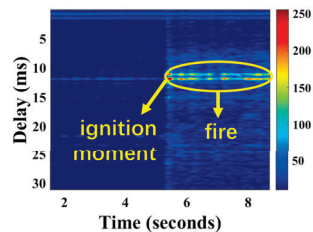


Fig. 3. CIR plot.

impossible to satisfy in practice. HearFire combines acoustic absorption and sound speed variations to detect early stage of fire, i.e., smoke, in indoor environments [33]. However, recent active acoustic-based works primarily focus on fire presence detection and do not investigate fire source localization and severity assessment, which are extremely important for emergency response to reduce casualties and property losses.

Challenges. In this paper, we propose UltraFlame, an acoustic-based fire monitoring system devoting to fill the gap of existing fire monitoring system. However, implementing such two crucial functionalities of fire monitoring using proactively emitted acoustic signals presents enormous challenges. The fundamental challenge of localizing fire sources involves how to measure acoustic signals affected by flames and determining the source's position. Since fire does not reflect sound waves [2], current methods to detect fire presence rely on acoustic signals that penetrate flames and reflect from objects behind the fire [33]. These methods compare the emitted and residual sound energy after being absorbed by the fire, allowing for accurate detection of the presence of flames. However, intuitively, sound waves that penetrate fires do not provide information about the location of the fire source. Regardless of where the fire source is positioned between the acoustic devices and the reflecting object, the energy absorption pattern penetrating fire is consistent, indicating only the amount of energy lost during the round trip. Therefore, achieving fire source localization using acoustic signals is a nontrivial task.

The second challenge lies in how to establish a reliable correlation between fire severity and sound propagation. Fire combustion is a highly dynamic process involving multiple complicated factors, including the nature of the combustible material, flame shape, temperature, etc. These factors interact with each other and release a great amount of heat, forming an irregular and unstable heated region near the flame, making it challenging to accurately measure the fire severity. While sound energy absorption property can effectively detect the event of fire occurrence, it may lack the ability to correlate with fire severity due to its randomness characteristic caused by complex and incomplete fire combustion.

Solutions. To address the first challenge, we conduct an in-depth study of the multi-path propagation characteristics of acoustic waves in indoor environments when fire source appears at different locations, and synthetically design a deep learning framework to position fire sources. Fortunately, al-

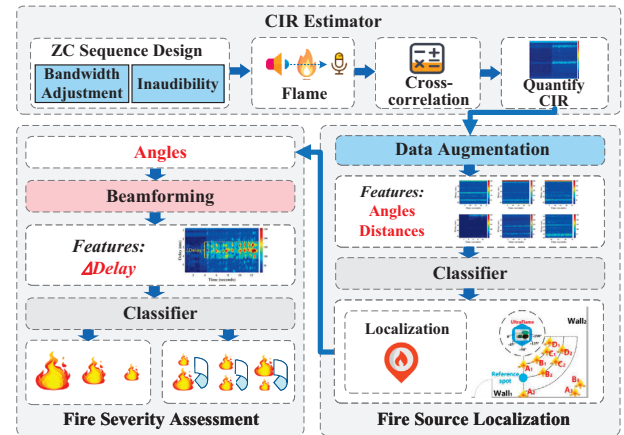


Fig. 4. Overview of UltraFlame.

though fire itself does not reflect any acoustic signal, the sound penetrating fire at different locations still encompasses reliable and detectable patterns in terms of sound absorption in indoor environments. Specifically, we observe distinct sound energy propagation patterns when fire is located at different distances and angles to the acoustic device, which significantly affects the acoustic channel measurements across multiple paths, resulting in varying sound intensities. Our extensive experiments demonstrate that fire sources located at different places, such as close to acoustic device, close to walls, and near a corner of a room, exhibit explicit and detectable nonlinear sound propagation characteristics. This in-depth analysis lays a solid foundation for accurate and interpretable data, facilitating us to apply a deep learning framework to establish a definite correlation between channel measurement and fire source positions. Our solution validates the feasibility of fire source localization using acoustic signals. We deliberately design a Vision Transformer (Vi-T) model to achieve accurate fire source localization.

To assess fire severity, we conduct a comprehensive analysis on sound propagation properties and dedicatedly quantify the relationship between the diameter of region where the heat is released by fire and the sound propagation delays. Such quantification is based on the fact that sound speed increases with elevating temperature. Our observation reveals that a larger flame generates a more extensive high-temperature area. As such, sound propagation can be more easily affected by the fire, resulting in a wider transmission delay range in channel measurement. Employing this correlation enables timely monitoring of fire impacted region, providing prompt feedback on the fire severity and accurate prediction of spreading tendency.

Contributions. In a nutshell, our main contributions are summarized as follows:

- We bridge the gap of existing fire detection system by implementing two crucial functionalities in fire monitoring systems. To the best of our knowledge, UltraFlame is the first system utilizing acoustic signals for pinpointing fire sources and assessing fire severity.
- Unlike existing methods that using signal reflection for

object localization, we prove that sound penetration still plays a crucial role in accurately pinpointing the fire source location. Moreover, we develop an innovative acoustic sensing metric to effectively assess fire severity.

- We implement a prototype of UltraFlame using low-cost commodity acoustic devices. Our experiments show that 94% of the localization results have an error of less than $0.8m$. Additionally, UltraFlame demonstrates an accuracy of 96.9% in assessing fire severity in indoor environments¹.

II. BACKGROUND

A. Fire Event Presence Detection Using Acoustic Signals

Existing acoustic-based approach, named HearFire [33], integrates a commercially available speaker and a microphone array, continuously emitting a predefined audio frame to sense the fire presence. The intuition is that sound energy can be absorbed by fire and sound speed increases with the elevated temperature. Zadoff-Chu (ZC) sequence is applied to probe the channel due to its high autocorrelation property, and cross-correlation based channel impulse response (CIR) estimation scheme is employed to measure the channel influenced by fire combustion.

CIR has been widely applied in acoustic sensing [15], [19], [27], [28], [30]–[32], enabling the granular segmentation of multipath signals into discrete bins or taps, each of which correlates to a specific range of propagation delays, as illustrated in Fig. 2. CIR $h[\tau]$ consists of complex values, profiling a comprehensive characterization of the attenuation of signals with different delays τ over time t . By isolating the bins that are exclusively affected by the targets of interest, it is possible to monitor the target by investigating fluctuations in signal delay and attenuation.

To achieve room-scale sensing while simultaneously maintaining the inaudibility of the emitted signal, HearFire exploits frequency domain interpolation scheme [27] on ZC sequence to extend its length and applies a dedicated parameter configuration scheme to maintain reliable sensing. The commodity speaker unceasingly emits the interpolated ZC sequence, part of whose energy will be absorbed by the heat released by fire. Such a sound energy absorption pattern can be captured by CIR measurement. Hearfire then removes the environmental interference and extracts the merely fire-impacted CIR using differential method on two adjacently received CIR traces. Fig. 3 shows the CIR measurements when fire is burning, which displays random variations in amplitude after igniting the fire, revealing a distinct pattern of signal absorption due to incomplete combustion. While effectively detecting fire event occurrence, the functionalities of fire source localization and severity assessment are not investigated in HearFire.

B. Fire Severity

Fire severity can be jointly characterized by variation in the energy released and the size of flame during the combustion process [7], which can be represented as:

¹Experiments were conducted with the presence of professional firefighters and were approved by the Institutional Review Board.

$$Fire_{Severity}(Q) \propto nC_pT_2 \quad (1)$$

where Q denotes the released heat of the flame, n is amount of substance, which represents the quantity of entities (such as molecules, atoms, or ions) contained in a substance. C_p is the specific heat capacity of a substance at constant pressure (i.e., atmospheric). T_2 is the temperatures during combustion. This implies that the released heat $Fire_{Severity}(Q)$ is directly proportional to T_2 .

In sound propagation, sound velocity is significantly impact by the temperature of transmission medium. In an ideal gas medium, the relationship between the sound speed v and temperature satisfies $v = \sqrt{\gamma RT/M}$ [14], where R is the molar gas constant with a value of 8.3145 J/mol , and γ represents the specific heat ratio of the gas, which is associated with its molecular structure. T is the absolute temperature. M is the molar mass of the gas. Let $z = \sqrt{\gamma R/M}$ is a constant value for a particular gas medium, therefore $v = v_0 \sqrt{\frac{T_2}{T_0}}$, where v_0 is the speed of sound at a reference temperature T_0 , and T_2 is the current temperature. Given $v = d/\tau$, where d is the travelling distance of sound, and τ is the corresponding delay, substituting the expression for the speed of sound, we obtain $\tau = k \sqrt{\frac{1}{T_2}}$ where $k = \frac{d\sqrt{T_0}}{v_0}$ is a constant. We can infer that τ is inversely proportional to $\sqrt{T_2}$, which implies that as $Fire_{Severity}(Q)$ increases, τ decreases, and vice versa.

III. SYSTEM DESIGN

A. Overview

Fig. 4 depicts the system overview of UltraFlame. UltraFlame consists of three modules. CIR estimator sequentially measures CIR between the emitted and received ZC sequences. The estimated CIR effectively captures and characterizes the variation in both energy and delay of the transmitted sound waves impacted by flames, which involve rich information about angle and distance of the fire source. Then, data augmentation module enlarges the dataset using a typically designed data augmentation scheme to relieve the burden of heavy manual data collection. The fire source localization module initially extracts key features from the augmented CIR for precise positioning. Subsequently, beamforming technique is applied toward the angle obtained from the localization process, facilitating further assessment of fire severity. Such design yields important insights into the fire's intensity and its potential spread.

B. Mining Distance and Angle Information in CIR

Fire occurrence can be detected using sound absorption characteristics, which, however, may miss the information on distance and angle of the fire source. Intuitively, fire appearing at any location between UltraFlame and wall tends to have the same energy absorption pattern in CIR since sound traverses the fire rather than being reflected from it. Nevertheless, in our work, we have a key observation that sound penetrating fire source at different locations manifests subtle but detectable

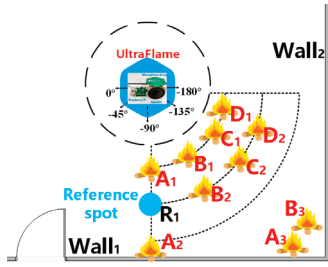


Fig. 5. Indoor fire source localization scenario.

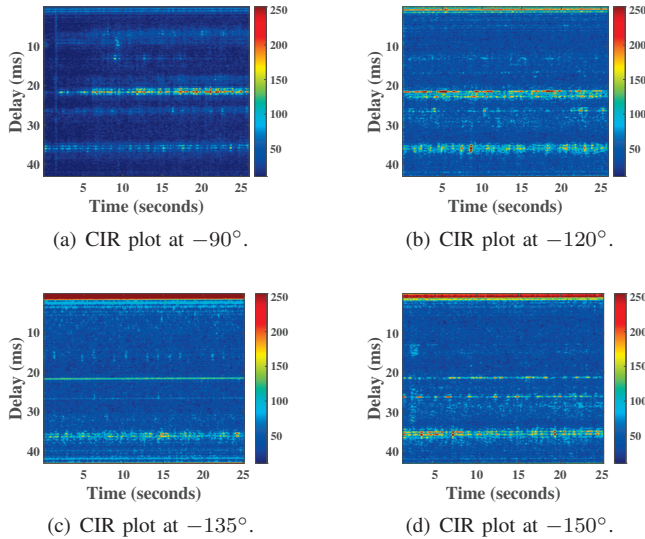


Fig. 6. Fire source at different angles.

discrepancies in sound energy absorption, which can still be captured by CIR if properly handled.

To validate this phenomenon, we conduct the following series of experiments. We place UltraFlame in the center of a room with a size of $7m \times 6m \times 3m$, as shown in Fig. 5. The speaker of UltraFlame is oriented perpendicularly to the concrete wall1. We assign this direction to -90° as reference angle. We first place a fire source in the Line-of-Sight (LOS) path between UltraFlame and wall1, which is 2m away to the UltraFlame (i.e., R1). The measured CIR when fire is burning at R1 is regarded as reference CIR, as shown in Fig. 6(a). The captured CIR measurements exhibit clear sound energy absorption pattern near 20ms delay, which is exactly the sound waves penetrating fire and being reflected back from the wall1 (i.e., 3.5 meters distance between UltraFlame and wall1). We then position the fire source at different distances and angles to UltraFlame and measure the CIR for each scenario. Insightful and rich information about fire source location can be observed in CIR plot. We explain it as follows in detail.

1) *Fire source at different angles to UltraFlame:* In this section, we delve into how different angles of fire to our UltraFlame impact the CIR measurements. In this scenario, we maintain a distance of 1m between the fire source and UltraFlame, while only varying the angle of the fire source relative to UltraFlame, such as -90° , -120° , -135° , and -150° , respectively, as R1, B1, C1, D1 shown in Fig. 5. The

fire source is placed on a thin metal surface to mitigate the reflection from the container. The corresponding CIR plots are depicted in Fig. 6.

From Fig. 6(b) to Fig. 6(d), we concentrate on two dominant CIR patterns. The first one lies in the CIR pattern around 20ms, which characterizes the LOS path between UltraFlame and wall1. The second one focuses on CIR measurements near 35ms, which exhibit the sound reflected by corner. Interestingly, as the angle of fire moves away from the LOS path (i.e., from -90° to -150°) between the device and the wall1, the dominance of CIR pattern near 20ms gradually diminishes. This is because sound waves propagating along LOS between UltraFlame and wall1 are less affected by the fire combustion with increasing angles. On the contrary, the CIR pattern near 35ms is increasingly pronounced since fire poses more remarkable effects on these parts of paths, yielding a more conspicuous energy absorption pattern. We note that the LOS transmission between speaker and microphone is not effectively removed at these three angles because energy variations on LOS transmission and caused by fire share the same level. To sum up, as the angle between fire and UltraFlame shifts, the sound propagation paths influenced by the flame undergo corresponding changes, which confirms that differences in the fire's angles indeed result in varying CIR measurements.

2) *Fire source at different distances to UltraFlame:* We then investigate the effects of different fire source distances. Typically, we study the impacts under three cases:

Case 1: We ignite the fire very close to UltraFlame, for instance, at a distance of 0.3m (i.e., A1). The measured CIR is shown in Fig. 7(a). The CIR plot exhibits a clear energy absorption pattern near the LOS transmission (i.e., at the top of CIR plot with lowest delays) between the speaker and microphone compared with that of R1. In this case, the LOS path is significantly affected by the heat released by combustion, incurring distinct absorption pattern in sound energy. Surprisingly, the signals reflected by wall1 (i.e., near 20ms delay) are absent throughout the experiment. This is because most of sound energy attenuates when penetrating fire, being reflected by wall and penetrating fire again back to the microphone. In other word, a fire close to UltraFlame absorbs the vast majority of sound energy, only exhibiting energy variation near LOS path. We keep the distance of fire at 0.3m while varying the angle to our UltraFlame (i.e., location B1, C1, and D1), the measured CIR plots show a similar pattern. Therefore, this pattern can serve as an indicator for specifying the approximate fire source location that close to the acoustic device.

Case 2: When the fire source appears very close to wall1, i.e., A2 in Fig. 5, part of the heated region generated by fire combustion is blocked by wall1, resulting in a relatively smaller high-temperature field compared with that at R1. As sound waves propagate penetrating this temperature field, the measured sound energy across different delays is more concentrated, as depicted in Fig. 7(b), manifesting more cohesive CIR patterns than R1 in Fig. 6(a). More importantly,

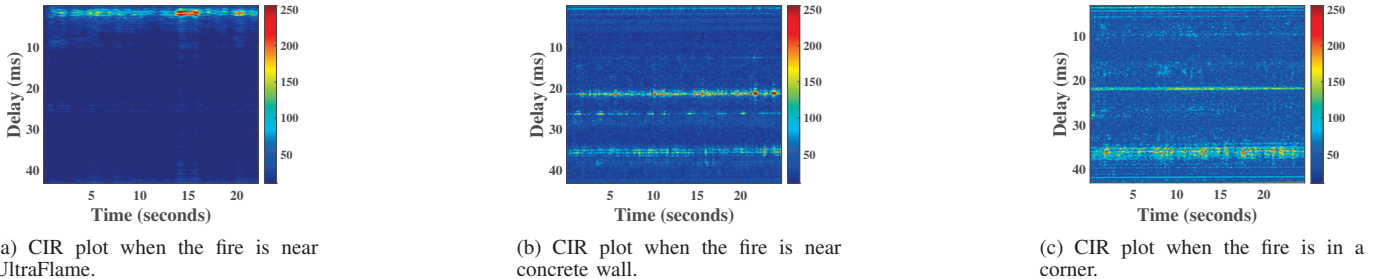


Fig. 7. Fire source at different distances.

the CIR variation in LOS path between the speaker and microphone is absent throughout the experiment, indicating a dominance of CIR variation caused by fire combustion over LOS transmission. Such unique patterns provide us with position information when the fire occurs near the wall.

Case 3: We measure the CIR when a fire is ignited near a room corner, i.e., A3 and B3 in Fig. 5, as depicted in Fig. 7(c). The LOS path between speaker and microphone is effectively canceled. CIR measurements at approximate 22ms delay manifest a relatively consistent energy pattern, which characterize the sound waves directly reflected by wall1. On the contrary, an unstable energy absorption pattern exhibited at 35ms delay indicates the signal path reflected in the corner and affected by the fire². We demonstrate that sound waves encountering complex interactions with the walls and flames near the corner engender rich multipaths, which are influenced by fire. Such a complicated interaction between sound waves and fire yields more chaotic energy absorption pattern, which profiles the information of fire source location near a corner.

The above three cases validates that CIR measurements contain rich information about distances of fire source, even if fire is incapable of reflecting the sound waves. Note that multipath in CIR provides valuable characteristics, such as reflections from walls and corners, which is essential for precise fire source localization.

3) Enlarging dataset using data augmentation: Our extensive experiments demonstrate a distinct nonlinear correlation between fire source location and CIR measurements. Such a nonlinear relationship prompts us to apply a deep learning framework to automatically extract these intricate nonlinear features and locating the fire source. However, neural networks demand a large-scale dataset covering diverse variations of CIR measured at different fire locations to guarantee accuracy and robustness. Data augmentation artificially increases the diversity and volume of training datasets, thereby enhancing the generalization capability of machine learning models and reducing overfitting. However, conventional data augmentation schemes, such as rotation, flipping, and affine of images cannot be applied to augment CIR measurements of flames, as they disrupt the temporal and spatial characteristics of CIR. Considering temporal dimension of CIR measurements, the CIR is measured frame by frame, precluding data augmentation along

²The propagation distance is approximately 12m, which is geometrically twice than the distances between our UltraFlame and the corner.

the X-axis, which distorts the temporal correlation of CIR measurements. Similarly, in terms of the spatial dimension, the CIR at different delays are strongly correlated with important location-related spatial information, including angles and distances. Therefore, potential transformations along the Y-axis of CIR plot may inherently be infeasible as well.

Different from classic data augmentation schemes, we dedicatedly devise the following data augmentation method to effectively expand the dataset. Specifically, we randomly vary the values of CIR measurements impacted by fire in a CIR plot. This is because complicated and incomplete fire combustion results in stochastic sound energy absorption, inducing random variations in CIR measurements. Note that we shift each fire-impacted CIR measurement within a certain range to somewhat retain its original intensity. The augmentation is performed on a per-frame basis (CIR trace), and the augmentation rate is empirically determined based on practical requirements. We utilize the augmented dataset in conjunction with the original dataset as inputs for the classifier.

C. Mining Fire Severity Information in CIR

After successfully locating the fire source, we utilize beam-forming technique to amplify signals from the identified angle of the ignition point, while eliminating interference from other directions. We then specifically extract information related to the severity of the fire from this angle. Recall that as the temperature elevates, the sound speed increases, resulting in a shorter propagation delay. Fire combustion, including even its early stages characterized merely by smoke, releases a large amount of heat, which engenders a high-temperature region near the flame. Such a high-temperature region accelerates the propagation of sound waves when encountering and penetrating it. Since fire combustion involves a series of complicated chemical and physical interactions, the distribution of temperature as well as the shape of this generated high temperature region is nonuniform, thereby yielding multiple sound copies with different delays.

1) Real-time fire severity monitoring: This complex region, however, can be quantitatively assessed via CIR, as depicted in Fig. 8. We observe multiple CIR measurements manifesting diverse delays near 3ms when igniting a fire after 4s at an equivalent distance of 0.5m from UltraFlame. Based on this observation, our core idea is that sound propagation can be more significantly affected by a larger high temperature region resulting in wider *Delay Range*. Therefore, we introduce a

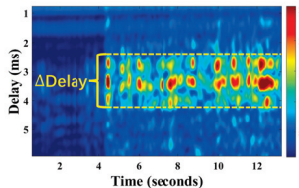


Fig. 8. Steady fire measurement.

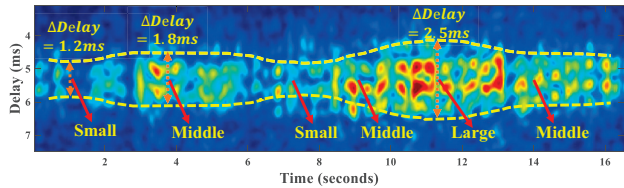


Fig. 9. Quantifying fire severity by analyzing sound wave delays in high-temperature fields.

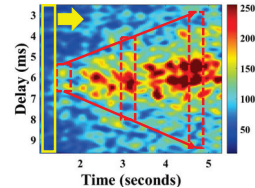


Fig. 10. Real-time capturing of fire severity.

novel metric, termed ΔDelay of CIR measurements characterizing the range of sound propagation delay between smallest and largest CIR measurements in CIR plot. ΔDelay estimates the diameter of the high temperature region caused by fire combustion, and therefore assesses fire severity.

To validate our observation, we conduct an experiment by maintaining the position of fire while manually varying the flame size. In our experiment, we manipulate the size of the high-temperature region by adjusting the valve of a gas stove. Specifically, we rigorously control the valve to ensure three distinct flame sizes. Fig. 9 illustrates CIR measurements under these three different flame sizes. The ΔDelay for small, medium, and large flames gradually increases, which covers the propagation delays of sound waves ranging 1.2ms , 1.8ms , and 2.5ms , respectively. As fire size increases, the high temperature field enlarges, resulting in a gradual expansion of ΔDelay . Such a key metric to measure fire severity offers us the potential to effectively predict the fire spreading tendency.

2) *Tracking fire spreading tendency:* In this validation, we gradually alter the valve of the gas stove from minimum to maximum in 3s to track the fire spreading tendency. The captured CIR measurements are illustrated in Fig. 10. From the moment of igniting fuels at the 1s to 4s , ΔDelay expands from the initial 1ms to 6.5ms . Our experiment convinces that ΔDelay can serve as an effective indicator for assessing fire severity, which is exploited to predict the fire spreading tendency. We employ a Sliding Window (SW) approach to monitor, as the yellow rectangle in Fig. 10. The window length is set to 5 (i.e., 5 CIR traces) to meet real-time requirements, and the sliding step of the SW is empirically set to 3. Utilizing the SW approach enables real-time measuring of ΔDelay , and thus predicting the fire spreading tendency.

D. Classifier

We employ the Vi-T model to extract features from CIR measurements for fire source localization and severity assessment [5]. The self-attention mechanism of Vi-T captures global context and analyzes CIR more effectively than traditional CNNs and RNNs, rendering it particularly suitable for identifying fire sources and combustion patterns with CIR pattern while enhancing training efficiency. For fire source localization, we partition the room into cubes and ignite fires at their centers. We augment CIR measurements to classify fire severity based on flame size. Vi-T processes consecutive CIR traces to output 3-D coordinates and fire size. Its self-attention mechanism autonomously selects relevant CIR pat-

terns, ensuring accurate positional information and effective fire assessment, even in the presence of varying reflections.

Therefore, we configure the Vi-T as follows. The input of our classifier is a CIR plot with a size of $H \times W$, where H is height and W is width, respectively. Convolution is performed with 768 kernels to extract features from the image, which are then flattened to yield a 196×768 matrix. Through concatenation, this matrix is combined with a 1×768 classification feature vector to form a 197×768 matrix, followed by positional encoding. After passing through Extract Class Token layers, a 1×768 classification feature vector is extracted. This vector is then input into two sets of MLP Head layer, producing two probability vectors of sizes $1 \times M$ and $1 \times N$, representing the classification ranks of fire locations and fire severity levels, respectively. The final classification results correspond to the category with the highest probability in each respective probability vector.

IV. EXPERIMENTS AND EVALUATION

A. Experiment setup

1) *Hardware:* The applied hardware in UltraFlame is shown in Fig. 11(a), which consists of a commercial speaker and circular microphone array. For precise acoustic signal transmission, UltraFlame uses Google AIY Voice Kit 2.0, integrating a 3W speaker controlled by a lightweight Raspberry Pi Zero. For effective signal reception, we apply the ReSpeaker 6-Mic Circular Array Kit with a 48kHz sampling rate, which accurately captures audio frames in the inaudible band. The cartridge stove used in the experiment is shown in Fig. 11(b).

2) *Data Collection:* We set the root ZC sequence with parameters $u = 64$ and $N_{zc} = 127$, and interpolate it to a length of $N'_{zc} = 2048$, which covers 7.25m in indoor environments. Data collection is conducted in three different rooms of varying layouts, with sizes of $4\text{m} \times 6\text{m} \times 3\text{m}$, $5\text{m} \times 5\text{m} \times 3\text{m}$, $7\text{m} \times 8\text{m} \times 3\text{m}$, respectively, as illustrated in Fig. 11(c)-11(e). UltraFlame is placed close to the wall while fire sources are positioned at different distances and angles to UltraFlame within a $0^\circ \sim 180^\circ$ area in front of UltraFlame. We manually collect 6,000 CIR plots, which are augmented by $100\times$ for fire source localization, severity assessment, and fire spreading tendency prediction. In addition to the controlled setting using a gas stove, we conduct an experiment to test UltraFlame's capability in tracking the tendency of fire spread. We apply a thin metal container with a size of $0.6\text{m} \times 0.2\text{m} \times 0.01\text{m}$ to mitigate container reflections. To achieve a flame size increase, we separately place four alcohol swipes straightly at intervals of 0.2m in the container interconnected by a piece of thread

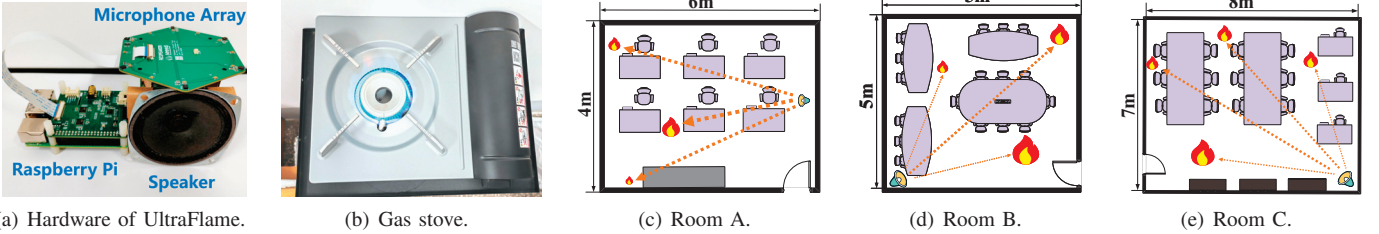


Fig. 11. Commercial speaker and microphone applied in UltraFlame and three rooms.

soaked in alcohol. The swipes are sequentially ignited via thread, representing a gradually fire expanding tendency.

3) Model Training and Testing: We take a less than 2s CIR plot as the input of the model, which covers 40 CIR traces. Therefore, the size of each input CIR plot is 40×2048 . The Vi-T model is trained and evaluated using PyTorch on a laptop equipped with a 32 GB memory, a 12th Generation Intel Core i7-12700H CPU, and an NVIDIA GeForce RTX 3060 Laptop GPU. The dataset is evenly split, allocating 50% for training and 50% for testing, respectively. We adopt a 10-fold cross-validation scheme for evaluation. The size of our trained model is less than 10M. Our test dataset includes data from other unseen rooms to meet the practical detection needs.

4) Benchmark: We select the state-of-the-art acoustic fire detection approach, HearFire [33], as the benchmark for comparison. We use the same hardware and experimental settings as in the HearFire. We employ the same fuel and transmission signals as in HearFire to detect fire occurrence since fire source localization and fire severity assessment are not available in HearFire. We also compare the processing delay between UltraFlame and HearFire.

B. Evaluation

1) Overall System Performance: We comprehensively evaluate the overall performance of UltraFlame. The training and testing dataset comprises both manually collected data and augmented data from three rooms. UltraFlame achieves an outstanding accuracy of 99.6% in detecting the occurrence of fire as shown in Fig. 12, with a false alarm rate of lower than 0.5%. This is due to the distinct feature of energy absorption when fire appears. Such an accurate value adequately ensures the reliability of the following tasks.

As illustrated in Fig. 13, over 94% of fires with unknown locations are accurately categorized within the same cube across all three rooms, indicating that 94% of the localization results achieve an error of less than 0.8m. We note that this localization error can be further reduced by subdividing the space into smaller cubes and employing more advanced neural networks. In our evaluation, the size of the partitioned cube is $1m \times 1m \times 1m$, which is adequate for effective fire monitoring in indoor environments. CIR measurements when fire source appears at a different location indeed effectively provide rich angle and distance information. The overall efficacy of the system in accurately distinguishing fire severity is depicted in Fig. 14. The average accuracy of assessing small, medium

and large flame achieves 96.9%, with all flame sizes exceeding 96.5%, demonstrating its ability to assess fire severity.

2) Performance of Localization with Different Angles and Distances: We randomly select 8 out of 15 cubes with different distances and angles to the acoustic device in Room B to ignite the fire, manually measuring 300 CIR plots at cube and applying a data augmentation with a factor of 100. Fig. 15 illustrates the confusion matrix of these 8 locations, which are labeled as $L1, L2 \dots L8$. UltraFlame achieves an average accuracy of 98% in distinguishing these 8 positions, with the accuracy for each location exceeding 96%. Such a promising performance certifies the capability of sound waves in localizing fire sources, even without reflection from the fire.

3) Performance of Fire Severity Assessment at Different Angles and Distances: We estimate the fire severity at different locations. We manually define the size of fire to small, medium and large implemented with different volumes of fuel, which generate corresponding sizes of the heated region. We ignite different fuels with varying volumes and collect the CIR measurements spanning across different distances and angles relative to UltraFlame. The augmentation is performed $100 \times$.

Fig. 16 illustrates the estimation accuracy for fire severity over 15 locations with different angles and distances. Fire severity can be accurately assessed with an accuracy of exceeding 94%. Due to multipath effect as well as rich temporal and spatial information in CIR measurements affected by fire combustion, different angles and distances pose limited influence on fire severity assessment. Our evaluation confirms that sound wave inherently involves the potential to effectively monitor the fire severity. The accuracy in fire severity determination at 15 different positions is consistently above 94.2%.

4) Performance on Different Heights: We evaluate whether varying the height of the ignition source impacts the performance of UltraFlame. To this end, we randomly select 6 locations in Room C and alter the heights of fire sources at each location: 0.5m, 1m, and 1.5m, respectively. Consequently, this results in 18 distinct ignition points. At each point, we measure 200 CIR plots, followed by applying a $100 \times$ augmentation.

We first estimate whether the height of fire will impact its localization accuracy. The result in Fig. 17 manifests that all points at different heights achieve an localization precision of over 94%. Different heights do not influence the performance of UltraFlame positioning the fire sources. This is because high temperature region incurred by fire combustion imposes significant impact on sound propagation, which can be effectively captured by CIR.

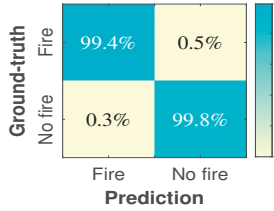


Fig. 12. Overall performance of fire occurrence detection.

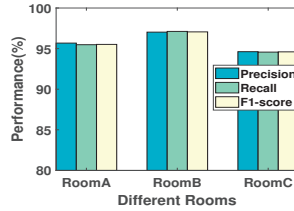


Fig. 13. Overall performance of fire source localization.

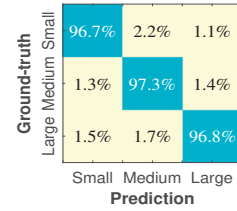


Fig. 14. Overall performance of fire severity assessment.

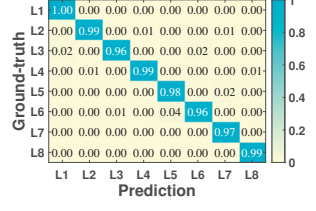


Fig. 15. Performance of localization with different angles and distances.

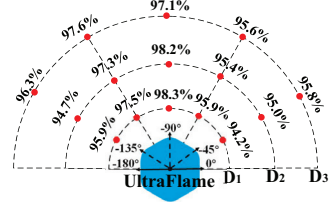


Fig. 16. Performance of fire severity assessment on different angles and distances.

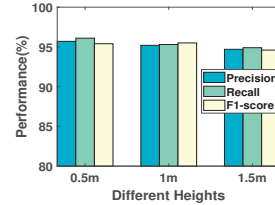


Fig. 17. Performance of localization at different heights.

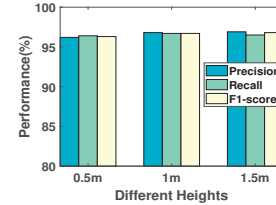


Fig. 18. Performance of fire severity assessment at different heights.

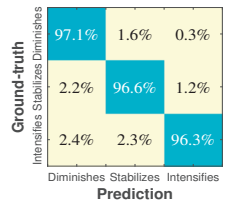


Fig. 19. Performance on fire severity prediction.

TABLE I
PERFORMANCE ON DIFFERENT CLASSIFIERS.

Classifier	APL	BPL	WPL	APS	BPS	WPS
CNN	93.2%	97.8%	91.5%	88.5%	91.7%	84.8%
RNN	94.0%	97.1%	93.3%	86.4%	89.5%	79.6%
Vi-T	95.7%	100%	94.3%	96.9%	98.3%	94.2%

We then assess fire severity at different heights. Fig. 18 demonstrates that an average accuracy of over 95% is achieved when determining fire severity at different heights for all ignition points. Such a reliable result benefits from our proposed effective metric characterizing the diameter of high-temperature region generated by fire combustion.

5) *Performance on Fire Severity Prediction:* We define three fire spreading tendencies, which are diminishing, stable and intensifying. To control fire spreading tendency, we place a thin metal lid on the top of container, which is slowly moved forward and backward using a fine metal wire to open and close the container. The flame size generated by fuel burned in the container will increase and decrease correspondingly. For each tendency, we measure 1000 CIR plots.

Fig. 19 plots the confusion matrix of these three tendencies. The average accuracy for fire severity prediction achieves 96.7% with each accuracy of tendency exceeding 96%. Due to complicated combustion reaction as well as irregular heated region, 2.4% and 2.2% of diminishing fire are wrongly predicted as intensifying and stable, respectively. Overall, UltraFlame can reliably predict the fire spreading tendency due to variation of delay range of sound waves.

6) *Performance on Different Classifiers:* To demonstrate the superiority of applying Vi-T, we evaluate UltraFlame using three different classifiers, including CNN, RNN and Vi-T. We use the same convolutional kernel size and number of layers to focus on performance on fire monitoring. Table I illustrates the system performance using different classifiers. APL, BPL and WPL represent Average Performance, Best Performance,

TABLE II
EXECUTION TIME.

Frame Detection	CIR Calculation (ms)			Fire Sensing (ms)		
	Down Conversion	CIR	Fire Occurrence Detection	Fire Source Localization	Fire Severity	
280	15	28	14	27	46	

Worst Performance of Fire Localization, respectively; APS, BPS, and WPS represent Average Performance, Best Performance and Worst Performance of Fire Severity, respectively. Our Vi-T model outperforms the other two models in all six indicators, especially in fire severity assessment. Its self-attention mechanism, large-scale pretraining, and ability to handle sequential data contribute to its superior performance.

7) *Execution Time:* Table II presents the processing time for each step in UltraFlame. In particular, frame detection is only performed once at the beginning when the first sound fame is received, although requiring 280ms. Processing delay for measuring the fire-affected CIR is 28ms. Surprisingly, the total time for the three fire sensing tasks is only 87ms. Fire severity assessment takes the longest detection time since it is more complicated than other two tasks, yielding a 46s to output an assessment result. Consequently, the overall processing delay for UltraFlame remains below 0.5s.

8) *Comparison with State-of-the-art Work:* We use HearFire [33] as a benchmark, which similarly relies on acoustic signals for fire detection. In Table III, APO, APL, APS and APP represents Average Performance of Fire Occurrence, Fire Source Localization, Fire Severity, and its Prediction, respectively. UltraFlame achieves a detection accuracy of 99.6% for fire occurrence, surpassing HearFire by 3.6% due to the use of the outstanding Vi-T classifier. Additionally, UltraFlame can fulfill fire source localization and severity assessment tasks, which are not available in HearFire. Moreover, it enables faster fire detection than HearFire, establishing itself as a more powerful acoustic-based fire sensing system.

TABLE III
COMPARISON WITH STATE-OF-THE-ART WORK.

	APO	APL	APS	APP	Detection Time
HearFire	96.0%	Not Supported	Not Supported	Not Supported	<0.7s
UltraFlame	99.6%	95.7%	96.9%	96.7%	<0.5s

V. RELATED WORK

A. Smoke Based Fire Detection

Smoke detectors have been widely applied to prevent fire disaster in our daily life [6], [8], [25], [29]. Smoke sensors can detect the smoke particles generated by fire [6], [25] and issue an alarm when the level of smoke exceeds a threshold. When a smoke level can be calculated by the photoelectric smoke sensor, which measures the difference in light dispersion with and without smoke using an optical device [8]. Another smoke detector applies an ionization chamber and a source of ionizing radiation to detect smoke when smoke particles enter the ionization chamber [29]. However, environmental impurities such as dirt, dust particles, and other air particles are prone to result in false alarms in photoelectric sensors, while ionization smoke detectors may present inhalation risks to humans due to the emission of radioactive materials during combustion.

B. Vision Based Fire Detection

Image-based fire detection systems utilize cameras to monitor fires and incorporates deep learning technologies for fire detection [4], [13], [20], [23], [40]. Celik et al. [40] employ the YCbCr color space to detect the flame, which effectively separates brightness from chrominance. Kozeki et al. [20] investigate the ability of a thermal camera system for detecting and monitoring burning fires and devise suitable image processing algorithms to extract combustion features. Chen et al. [4] showcase various aspects of fire detection using a fusion approach, including flame movement, color traces, and an algorithm for detecting flame flickering. However, the effectiveness of vision-based approaches for fire monitoring is limited by their reliance on unobstructed LOS paths [13], [22]. In addition, long time camera surveillance in indoor environment may raise privacy issues [9], [10].

C. Radio Frequency Based Fire Detection

Recent studies apply RF sensing to fulfill fire detection tasks [16], [26], [39]. Wi-Fire can detect fire in indoor environments using Wi-Fi sensing [39]. The intuition is that fire inflammation will impact the wireless channel, which can be revealed in the amplitude and phase of Channel State Information (CSI). However, access to CSI is unavailable for most of Wi-Fi network interface cards (NIC). Signals at the 28GHz frequency band can be potentially applied for fire detection due to the outstanding propagation properties and large sensing range and coverage [16]. Unfortunately, emitting signals with 28GHz requires specialized devices, which restrain their wide use. RFire enables through-wall fire detection using millimeter wave technology, and applies deep learning framework to extract instances of fire [26]. Nevertheless, RFire entails a 24s high-delay 3D spatial sweep for localizing the fire source,

which is hard to satisfy real-time requirement. However, RF-based methods either necessitate expensive specialized devices or are inaccessible in remote rural areas.

D. Acoustic Based Fire Detection

Using acoustic signals to detect fire can be roughly divided into two categories: passive [21], [24] and proactive fire sensing [3], [33], [38]. In passive fire sensing, recent works merely utilize microphones to passively capturing the sound produced during flame combustion. By analyzing the frequency and amplitude of the captured sound, the fire source location and fire severity can be identified [24]. Different materials during combustion result in unique acoustic emission (AE), pyrolysis and burning phases, which can be exploited to infer the presence of a fire event [21]. However, passive schemes are vulnerable to interference from ambient environmental noise [21], [24]. Proactive acoustic fire sensing detects the fire occurrence by actively emitting a predefined sound frame to probe the acoustic channel impact by fire combustion, therefore it is insensitive to environmental noises. Acoustic-Thermo sends an acoustic pulse to calculate air temperature based on sound speed. However, it suffers from precise system initialization by measuring the round trip distance to a pre-deployed barrier before use [38]. AcuTe+ applies commodity speaker and microphone to monitor the ambient temperature with a measurable range of only from 5°C – 38°C [3]. HearFire combines acoustic energy absorption and sound speed variation caused by fire burning to accurately identify fire occurrence indoors [33]. Recent proactive acoustic-based approaches focus on detecting fires. Unlike these, UltraFlame provides fire source localization and severity assessment, significantly advancing emergency response design.

VI. CONCLUSION

We introduce UltraFlame, an indoor fire monitoring system that effectively addresses practical challenges associated with capturing reliable fire location patterns without any reflection from flame. Furthermore, we introduce an innovative metric to correlate the fire severity with sound propagation delays for precise fire severity assessment. Extensive experiments demonstrate that 94% of the localization results have an error of less than 0.8m. Additionally, UltraFlame achieves an accuracy of 96.9% in fire severity assessment in indoor environment. UltraFlame offers real-time fire monitoring, contributing to timely prediction and efficient rescue operations. It is a huge step forward for modern fire rescue systems, which aims to bridge the gap of existing fire monitoring systems and integrate embodied intelligence for enhanced adaptive responses.

ACKNOWLEDGMENT

This work is supported by the Science and Technology Innovation Program of Hunan Province under Grant 2024RC3105, the Natural Science Foundation of Hunan Province of China under Grant 2023JJ20015, the Guangdong Basic and Applied Basic Research Foundation under Grant 2024A1515011687, the Shenzhen Science and Technology Program under Grant JCYJ20240813162405008, and the Hong Kong GRF under Grant PolyU 15211924.

REFERENCES

- [1] B. C. Arrue, A. Ollero, and J. M. De Dios. An intelligent system for false alarm reduction in infrared forest-fire detection. *IEEE Intelligent Systems and their Applications*, 15(3):64–73, 2000.
- [2] M. I. Boulos. Flow and temperature fields in the fire-ball of an inductively coupled plasma. *IEEE Transactions on Plasma Science*, 4(1):28–39, 1976.
- [3] C. Cai, H. Pu, L. Ye, H. Jiang, and J. Luo. Active acoustic sensing for “hearing” temperature under acoustic interference. *IEEE Transactions on Mobile Computing*, 22(2):661–673, 2023.
- [4] J. Chen, Y. He, and J. Wang. Multi-feature fusion based fast video flame detection. *Building and Environment*, 45(5):1113–1122, 2010.
- [5] A. Dosovitskiy, L. Beyer, A. Kolesnikov, D. Weissenborn, X. Zhai, T. Unterthiner, M. Dehghani, M. Minderer, G. Heigold, S. Gelly, J. Uszkoreit, and N. Houlsby. An image is worth 16x16 words: Transformers for image recognition at scale. *CoRR*, abs/2010.11929, 2020.
- [6] D. D. Drysdale. *Thermochemistry*, pages 138–150. Springer New York, New York, NY, 2016.
- [7] C. Gao, J. Cong, Y. Sun, D. Han, and G. Wang. Variability in pyrogenic carbon properties generated by different burning temperatures and peatland plant litters: implication for identifying fire intensity and fuel types. *International Journal of Wildland Fire*, 31(4):395–408, 2022.
- [8] A. Gaur, A. Singh, A. Kumar, K. S. Kulkarni, S. Lala, K. Kapoor, V. Srivastava, A. Kumar, and S. C. Mukhopadhyay. Fire sensing technologies: A review. *IEEE Sensors Journal*, 19(9):3191–3202, 2019.
- [9] S. Gregory. Cameras Everywhere: Ubiquitous Video Documentation of Human Rights, New Forms of Video Advocacy, and Considerations of Safety, Security, Dignity and Consent. *Journal of Human Rights Practice*, 2(2):191–207, 05 2010.
- [10] T. W. Hnat, V. Srinivasan, J. Lu, T. I. Sookoor, R. Dawson, J. Stankovic, and K. Whitehouse. The hitchhiker’s guide to successful residential sensing deployments. In *Proceedings of the 9th ACM Conference on Embedded Networked Sensor Systems*, SenSys ’11, page 232–245, New York, NY, USA, 2011. Association for Computing Machinery.
- [11] T. Islam, H. A. Rahman, and M. A. Syrus. Fire detection system with indoor localization using zigbee based wireless sensor network. In *2015 international conference on informatics, electronics & vision (ICIEV)*, pages 1–6. IEEE, 2015.
- [12] X. Jin, X. Xie, K. An, Q. Wang, and J. Guo. Lora indoor localization based on improved neural network for firefighting robot. In *International Conference on Neural Information Processing*, pages 355–362. Springer, 2019.
- [13] J. M. Kahn, R. H. Katz, and K. S. J. Pister. Emerging challenges: Mobile networking for “smart dust”. *Journal of Communications and Networks*, 2(3):188–196, 2000.
- [14] V. Kytin and G. Kytin. Analysis of the shape of acoustic signal frequency responses while determining absolute temperature. *Measurement Techniques*, 59(1):62–66, 2016.
- [15] D. Li, J. Liu, S. I. Lee, and J. Xiong. Lasense: Pushing the limits of fine-grained activity sensing using acoustic signals. 6(1), mar 2022.
- [16] J. Li, A. Sharma, D. Mishra, and A. Seneviratne. Fire detection using commodity wifi devices. In *2021 IEEE Global Communications Conference (GLOBECOM)*, pages 1–6, 2021.
- [17] J. Li, Z. Xie, X. Sun, J. Tang, H. Liu, and J. A. Stankovic. An automatic and accurate localization system for firefighters. In *2018 IEEE/ACM Third International Conference on Internet-of-Things Design and Implementation (IoTDI)*, pages 13–24. IEEE, 2018.
- [18] N. Li, B. Becerik-Gerber, B. Krishnamachari, and L. Soibelman. A bim centered indoor localization algorithm to support building fire emergency response operations. *Automation in Construction*, 42:78–89, 2014.
- [19] K. Ling, H. Dai, Y. Liu, A. X. Liu, W. Wang, and Q. Gu. Ultragesture: Fine-grained gesture sensing and recognition. *IEEE Transactions on Mobile Computing*, 21(7):2620–2636, 2022.
- [20] Z. Liu and A. K. Kim. Review of recent developments in fire detection technologies. *Journal of Fire Protection Engineering*, 13(2):129–151, 2003.
- [21] J. Martinsson, M. Runefors, H. Frantzich, D. Glebe, M. McNamee, and O. Mogren. A novel method for smart fire detection using acoustic measurements and machine learning: Proof of concept. *Fire Technology*, 58(6):3385–3403, Nov. 2022.
- [22] J.-i. Meguro, T. Murata, J.-i. Takiguchi, Y. Amano, and T. Hashizume. Gps multipath mitigation for urban area using omnidirectional infrared camera. *IEEE Transactions on Intelligent Transportation Systems*, 10(1):22–30, 2009.
- [23] K. Muhammad, J. Ahmad, and S. W. Baik. Early fire detection using convolutional neural networks during surveillance for effective disaster management. *Neurocomputing*, 288:30–42, 2018. Learning System in Real-time Machine Vision.
- [24] K.-H. Park and S. Q. Lee. Early stage fire sensing based on audible sound pressure spectra with multi-tone frequencies. *Sensors and Actuators A: Physical*, 247:418–429, 2016.
- [25] E. Perera and D. Litton. A detailed study of the properties of smoke particles produced from both flaming and non-flaming combustion of common mine combustibles. *Fire Safety Science*, 10:213–226, 01 2011.
- [26] D. Radke, O. Abasi, T. Brecht, and K. Larson. Can future wireless networks detect fires? In *Proceedings of the 7th ACM International Conference on Systems for Energy-Efficient Buildings, Cities, and Transportation*, BuildSys ’20, page 286–289, New York, NY, USA, 2020. Association for Computing Machinery.
- [27] K. Sun, T. Zhao, W. Wang, and L. Xie. Vskin: Sensing touch gestures on surfaces of mobile devices using acoustic signals. In *Proceedings of the 24th Annual International Conference on Mobile Computing and Networking*, MobiCom ’18, page 591–605, New York, NY, USA, 2018. Association for Computing Machinery.
- [28] M. Tian, Y. Wang, Z. Wang, J. Situ, X. Sun, X. Shi, C. Zhang, and J. Shen. Remotegesture: Room-scale acoustic gesture recognition for multiple users. In *2023 20th Annual IEEE International Conference on Sensing, Communication, and Networking (SECON)*, pages 231–239, Sep. 2023.
- [29] M. Vojtisek-Lom. Total diesel exhaust particulate length measurements using a modified household smoke alarm ionization chamber. *Journal of the Air & Waste Management Association*, 61(2):126–134, 2011.
- [30] P. Wang, R. Jiang, and C. Liu. Amaging: Acoustic hand imaging for self-adaptive gesture recognition. In *IEEE INFOCOM 2022 - IEEE Conference on Computer Communications*, pages 80–89, May 2022.
- [31] W. Wang, A. X. Liu, and K. Sun. Device-free gesture tracking using acoustic signals. In *Proceedings of the 22nd Annual International Conference on Mobile Computing and Networking*, MobiCom ’16, page 82–94, New York, NY, USA, 2016. Association for Computing Machinery.
- [32] Y. Wang, J. Shen, and Y. Zheng. Push the limit of acoustic gesture recognition. In *IEEE INFOCOM 2020 - IEEE Conference on Computer Communications*, pages 566–575, July 2020.
- [33] Z. Wang, Y. Wang, M. Tian, and J. Shen. Hearfire: Indoor fire detection via inaudible acoustic sensing. *Proc. ACM Interact. Mob. Wearable Ubiquitous Technol.*, 6(4), jan 2023.
- [34] Q. Yang, K. Cui, and Y. Zheng. Room-scale voice liveness detection for smart devices. *IEEE Transactions on Dependable and Secure Computing*, 2024.
- [35] Q. Yang and Y. Zheng. Deepair: Sound localization with binaural microphones. *IEEE Transactions on Mobile Computing*, 23(1):359–375, 2022.
- [36] Q. Yang and Y. Zheng. Aquahelper: Underwater sos transmission and detection in swimming pools. In *Proceedings of the 21st ACM Conference on Embedded Networked Sensor Systems*, pages 294–307, 2023.
- [37] H. Yar, T. Hussain, M. Agarwal, Z. A. Khan, S. K. Gupta, and S. W. Baik. Optimized dual fire attention network and medium-scale fire classification benchmark. *IEEE Transactions on Image Processing*, 31:6331–6343, 2022.
- [38] F. Zhang, K. Niu, X. Fu, and B. Jin. Acoustithermo: Temperature monitoring using acoustic pulse signal. In *2020 16th International Conference on Mobility, Sensing and Networking (MSN)*, pages 683–687, Dec 2020.
- [39] S. Zhong, Y. Huang, R. Ruby, L. Wang, Y.-X. Qiu, and K. Wu. WiFire: Device-free fire detection using wifi networks. In *2017 IEEE International Conference on Communications (ICC)*, pages 1–6, May 2017.
- [40] T. Çelik and H. Demirel. Fire detection in video sequences using a generic color model. *Fire Safety Journal*, 44(2):147–158, 2009.